

RESEARCH ARTICLE

Rejuvenation of aged rat skin with pulsed electric fields

Xiaoxiang Li^{1,2} | Nima Saeidi¹ | Martin Villiger³ | Hassan Albadawi⁴ | Jake D. Jones⁵ | Kyle P. Quinn⁵ | William G. Austin Jr⁶ | Alexander Golberg^{1,7}  | Martin L. Yarmush^{1,8}

¹Center for Engineering in Medicine, Department of Surgery, Massachusetts General Hospital, Harvard Medical School, and the Shriners Burns Hospital, Boston, Massachusetts

²Orthopedics Oncology Institute of Chinese PLA, Department of Orthopedics, Tangdu Hospital, the Fourth Military Medical University, Xi'an, Shaanxi, China

³Wellman Center for Photomedicine, Massachusetts General Hospital, Harvard Medical School, Boston, Massachusetts

⁴Division of Vascular and Endovascular Surgery, Massachusetts General Hospital, Harvard Medical School, Boston, Massachusetts

⁵Department of Biomedical Engineering, University of Arkansas, Fayetteville, Arkansas

⁶Department of Surgery, Division of Plastic and Reconstructive Surgery, Massachusetts General Hospital, Harvard Medical School, Boston, Massachusetts

⁷Porter School of Environmental and Earth Sciences, Tel Aviv University, Tel Aviv, Israel

⁸Department of Biomedical Engineering, Rutgers University, Piscataway, New Jersey

Correspondence

Alexander Golberg, Porter School of Environmental and Earth Sciences, Tel Aviv University, Tel Aviv 69978, Israel.
Email: agolberg@tauex.tau.ac.il

Martin L. Yarmush, Center for Engineering in Medicine, Department of Surgery, Massachusetts General Hospital, 51 Blossom Street, Room 405, Boston, MA 02114.
Email: ireis@sbi.org

Funding information

National Natural Science Foundation of China, Grant/Award Number: 81402574; United States-Israel Binational Science Foundation; Shriners, Grant/Award Number: 85120-BOS

Abstract

The demand for skin rejuvenation procedures has progressively increased in the past decade. Additionally, clinical trials have shown that current therapies might cause downtime and side effects in patients including prolonged erythema, scarring, and dyspigmentation. The goal of this study was to explore the effect of partial irreversible electroporation (pIRE) with pulsed electric fields in aged skin rejuvenation as a novel, non-invasive skin resurfacing technique. In this study, we used an experimental model of aged rats. We showed that treatment with pIRE promoted keratinocyte proliferation and blood flow in aged rat skin. We also found significant evidence indicating that pIRE reformed the dermal extracellular matrix (ECM). Both the collagen protein and fibre density in aged skin increased after pIRE administration. Furthermore, using an image-processing algorithm, we found that the collagen fibre orientation in the histological sections did not change, indicating a lack of scar formation in the treated areas. The results showed that pIRE approach could effectively stimulate keratinocyte proliferation, ECM synthesis, and angiogenesis in an aged rat model.

KEYWORDS

aged skin, electroporation, partial irreversible electroporation, pulsed electric field, skin rejuvenation

1 | INTRODUCTION

As the largest organ of the human body, the skin exerts protective, immunological, thermoregulatory, and sensory functions. Skin aging is the result of two biological processes: photoaging and chronological aging. Both photoaging and chronological aging share important

molecular features, including structural and functional alterations, such as poor re-epithelialization, poor blood supply, and reduced collagenesis (Fisher et al., 2002). Consequently, aged skin is characterized by wrinkles, dryness, laxity, and elevated pigmentation (Fernandes et al., 2013). Currently, there is a high demand for skin rejuvenation practices. In 2016, in the United States, dermatological

Abbreviations: ECM, Extracellular matrix; EGF, Epidermal growth factor; H&E, Haematoxylin and eosin; IL-10, Interleukin 10; PEFs, Pulsed electric fields; VEGF, Vascular endothelial growth factor

surgeons performed nearly 10.5 million medically necessary or cosmetic procedures, an increase of 27% since 2012; these procedures involved skin rejuvenation via laser-, light-, and energy-based procedures; chemical peels; and microdermabrasion (American Society for Dermatologic Surgery (ASDS), 2016).

Skin rejuvenation therapies ideally aim to remove nonfunctional tissue and induce keratinocyte proliferation, extracellular matrix (ECM) synthesis, and angiogenesis, thus restoring a youthful appearance (Nand & Riyal, 2014; Quan & Fisher, 2015). Various techniques have been developed to achieve these effects (Badin et al., 2001; Hoenic & Hoenic, 2013; Lee et al., 2014; Mulholland, 2011; Savoia, Landi, & Baldi, 2013; Seo, Kim, Lee, Yoon, & Lee, 2013). Currently, most skin rejuvenation procedures have centred on those that destroy the epidermis and cause a dermal wound, resulting in dermal collagen remodelling, secondary skin tightening, and rhytid improvement. However, there is a wide range of significant side effects. Complications, such as prolonged erythema, scarring, dyspigmentation, and downtime, are still the major disadvantage of current procedures (Avram, Tope, Yu, Szachowicz, & Nelson, 2009; Cox & Adigun, n.d.; Park, Ahn, Choi, Kim, & Lee, 2012).

Exploration to uncover the next generation of skin rejuvenation treatments is being pursued to engineer therapies that further improve the texture and appearance of skin with minimal downtime and complications. One of these applications is electroporation, induced by a calibrated pulsed electric field (PEF) that modulate transmembrane potential of cell membranes (Neumann & Rosenheck, 1972). The strength of this physical approach is that cell membrane perturbation is perfectly controlled in the time because the PEF-induced permeabilization of cell membranes occurs solely in the tissue located in between electrodes. The application of PEFs also leads to cell reversible electroporation, cell irreversible electroporation, and death most probably through both necrosis and apoptosis, degranulation of mast cells, and release of multiple molecular factors to the treated areas at the time of treatment and up to days after the electric field was removed (Gibot & Golberg, 2016). Proteins and DNA synthesis were showed to be promoted by PEF (Bourguignon, Jy, & Bourguignon, 1989). On a tissue level, it was shown that electric fields increase the permeability of small molecules, DNA and RNA, into the skin (Pavšelj & Miklavčič, 2008; Yarmush, Golberg, Serša, Kotnik, & Miklavčič, 2014). This increase in skin permeability suggested the use of electroporation for needless drug delivery and for DNA vaccination applications (Gibot & Golberg, 2016; Yarmush et al., 2014). An additional effect of electric fields on the skin is the modulation of the blood flow. Studies on electrochemotherapy of tumours and normal skin showed that PEFs cause temporary vasoconstriction and then vasodilation at the treated areas (Yarmush et al., 2014). We have reported that partial irreversible electroporation (pIRE) induced by PEFs can rejuvenate skin in young rats (Golberg et al., 2015).

Although PEFs can kill (Davalos, Mir, & Rubinsky, 2005) and injure cells (Golberg et al., 2016), they preserve the ECM architecture. What is more, the permanent nanoscale defects permit molecules, such as growth factors, to come out from the targeted cells, and the locally released multiple growth factors induce new cell and tissue growth (Golberg, Broelsch, et al., 2013; Golberg, Bruinsma,

Jaramillo, Yarmush, & Uygun, 2016; Golberg et al., 2017; Golberg, Khan, et al., 2015; Phillips, Narayan, Padath, & Rubinsky, 2012; Rubinsky, Onik, & Mikus, 2007). This combination is the main characteristic of the technique, which is different from current skin rejuvenation procedures. Our previous results suggested that pIRE could produce re-epithelialization and improve skin function in young rats (Golberg, Khan, et al., 2015). However, aged patients rather than young patients need cosmetic procedures, and tissue repair differs between young and aged animals (de Melo Rambo et al., 2014; Reed, Karres, Eyman, Vernon, & Edelberg, n.d.). The goal of this paper is to explore whether pIRE can create the rejuvenation effect in aged animals and thus potentially serve as a novel, non-invasive skin resurfacing technique.

2 | MATERIALS AND METHODS

2.1 | Animals

Twelve-month-old female Sprague-Dawley rats ($N = 28$) were purchased from Charles River Laboratories (Wilmington, MA). The animals were housed in cages with two animals per cage with access to food and water ad libitum and were maintained on a 12-hr light/dark cycle in a temperature-controlled room. All animal procedures were approved by the Subcommittee on Research Animal Care of the Massachusetts General Hospital (protocol number 2012N000077) and were in accordance with the guidelines of the National Institutes of Health (NIH).

2.2 | Partial irreversible electroporation

Prior to pIRE administration, animals were anaesthetized with isoflurane. Their fur was clipped along the dorsal surfaces and wet with tap water (Figure 1). For each animal, six designated areas were treated with PEFs using contact electrodes over a surface area of 1 cm^2 (Figure 2a). The distances between the areas were greater than 0.5 cm. Tattoos were used to label the areas. Pulses were delivered using a BTX 830 pulse generator (Harvard Apparatus Inc., Holliston, MA). The following PEF settings were used: 200 pulses, 70- μs pulse duration, 3-Hz pulse frequency, and applied voltages of 500, 250, and 125 V. The gap between the electrodes was 2 mm.

2.3 | Laser Doppler scanning

A laser Doppler imager (Moor Instruments, Wilmington, DE) was used to assess blood flow. The laser Doppler source was mounted on a movable rack exactly 20 cm above the dorsum of the rat after the animal was anaesthetized and restrained on the underlying table. The laser beam (780 nm) reflected from circulating red blood cells in the capillaries, arterioles, and venules and was detected and processed to provide a computerized, colour-coded image. Image analysis software (Laser Doppler Perfusion Measure, Version 3.08; Moor Instruments) calculated the mean flux values representing the blood flow from the relative flux units for the areas corresponding to the rat dorsum. Baseline images were obtained from each rat before the

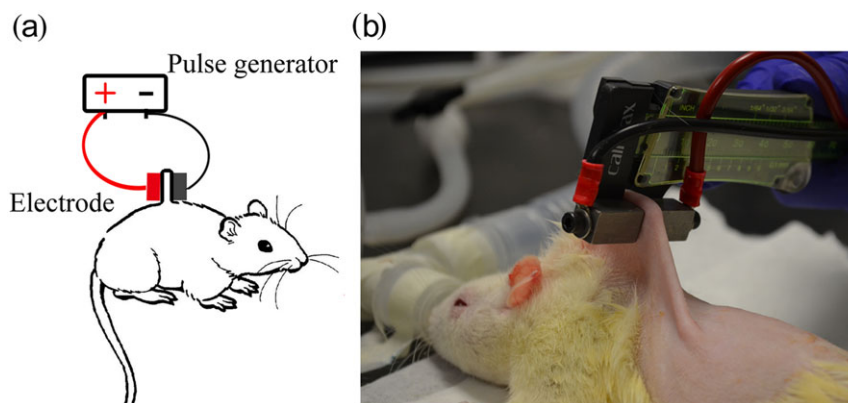


FIGURE 1 (a) Schematic representation of the experimental set-up and digital image of the electrodes used for partial irreversible electroporation administration. (b) Digital image of the treated rat [Colour figure can be viewed at wileyonlinelibrary.com]

treatment was administered. Then, the rats were treated with pIRE, and serial laser Doppler images were subsequently obtained. Skin perfusion was expressed as the ratio of the flux value of the treated area relative to the value of the same spot before treatment (Flux Ratio), which was verified by the tattoo that marked the point.

2.4 | Histology

Specimens were harvested 1 day, 3 days, 1 week, 3 weeks, 5 weeks, and 2 months following the initial pIRE administration. Four animals were euthanized at each time point. Four 12-month-old rats were used as controls. Skin samples were fixed in 10% formalin, embedded in paraffin, and cut into 7- μ m sections. Sections were stained with haematoxylin and eosin and Masson's trichrome. Tissues were processed and stained by the Rodent Histopathology Core at Harvard Medical School. Three separate investigators, including an experienced dermatopathologist, evaluated the slides in a blinded fashion. Colour images of each entire tissue section were acquired using a NanoZoomer Digital Pathology System (NanoZoomer 2.0-HT slide scanner; Hamamatsu, Hamamatsu City, Japan). To quantify the effects of pIRE on the thickness of the epidermis, we measured the distance between the basement membrane and the stratum corneum at a minimum of 20 points in four histological sections that were obtained from different animals sacrificed at the same time point.

2.5 | Automated image analysis

As described in previous studies, automated image analysis of the trichrome stain was performed to evaluate the fibre density and orientation (Quinn et al., 2014). Briefly, collagen fibres were identified from the images by blue-to-red intensity ratios exceeding 2. The local fibre density was determined by the relative number of collagen-positive pixels within a 50-pixel radius. The fibre orientation surrounding each image pixel was also computed, and directional statistics were employed to compute the local directional variance of the fibres within a 50-pixel radius. The directional variance provided a metric that was inversely proportional to the strength of fibre alignment in the average fibre direction. Subregions of 300 \times 700 μ m corresponding to the centre of the pIRE-treated tissue region were defined via blinded evaluation of the original trichrome images, and the average fibre density and directional variance were computed for each

subregion. For controls, we used the values from subregions from untreated skin tissue.

2.6 | Total collagen analysis

Specimens were snap-frozen in liquid nitrogen and stored at -80°C until analysis. After the tissue was weighed, 100 μ l of 6 M of HCl was added, and the tissue was hydrolysed at 95°C for 20 hr. Hydroxyproline was measured using the QuickZyme Total Collagen Assay (QuickZyme BioSciences, Leiden, The Netherlands) following the manufacturer's protocol.

2.7 | Immunohistochemistry

Staining for Ki-67 was performed on paraffin-embedded tissue sections. The sections were de-paraffinized, antigens were retrieved in citrate buffer (pH = 6.0), and the sections were blocked in normal goat serum and incubated overnight at 4°C in primary antibody (rabbit polyclonal Ki-67, 1:150 dilution, Abcam, Cambridge, MA). The sections were then stained in secondary rabbit anti-goat IgG (Vector Labs, Burlingame, CA), followed by phosphate-buffered saline washing and colour retrieval using DAB chromogen (Dako, Santa Clara, CA). The sections were dehydrated, counterstained using haematoxylin, rinsed in xylene, and coverslipped with cyto seal. Colour images of each entire tissue section were acquired using a NanoZoomer Digital Pathology System (NanoZoomer 2.0-HT slide scanner, Hamamatsu, Hamamatsu City, Japan). The slides were stained in one batch to eliminate artifactual variations. Quantitative analysis was performed by counting positively stained cells in five different fields of view at the highest possible resolution (80 \times). The percentage of positively stained cells was then determined in triplicate and compared with that measured for the control group.

2.8 | Statistics

Statistical analysis was performed using GraphPad Prism 6 and Microsoft Excel. The data are reported as the mean \pm standard error of the mean. Statistical analysis was performed by first using two-way analysis of variance for multivariate analysis followed by Tukey tests to assess the significance between individual groups. Significance was set at $p < 0.05$.

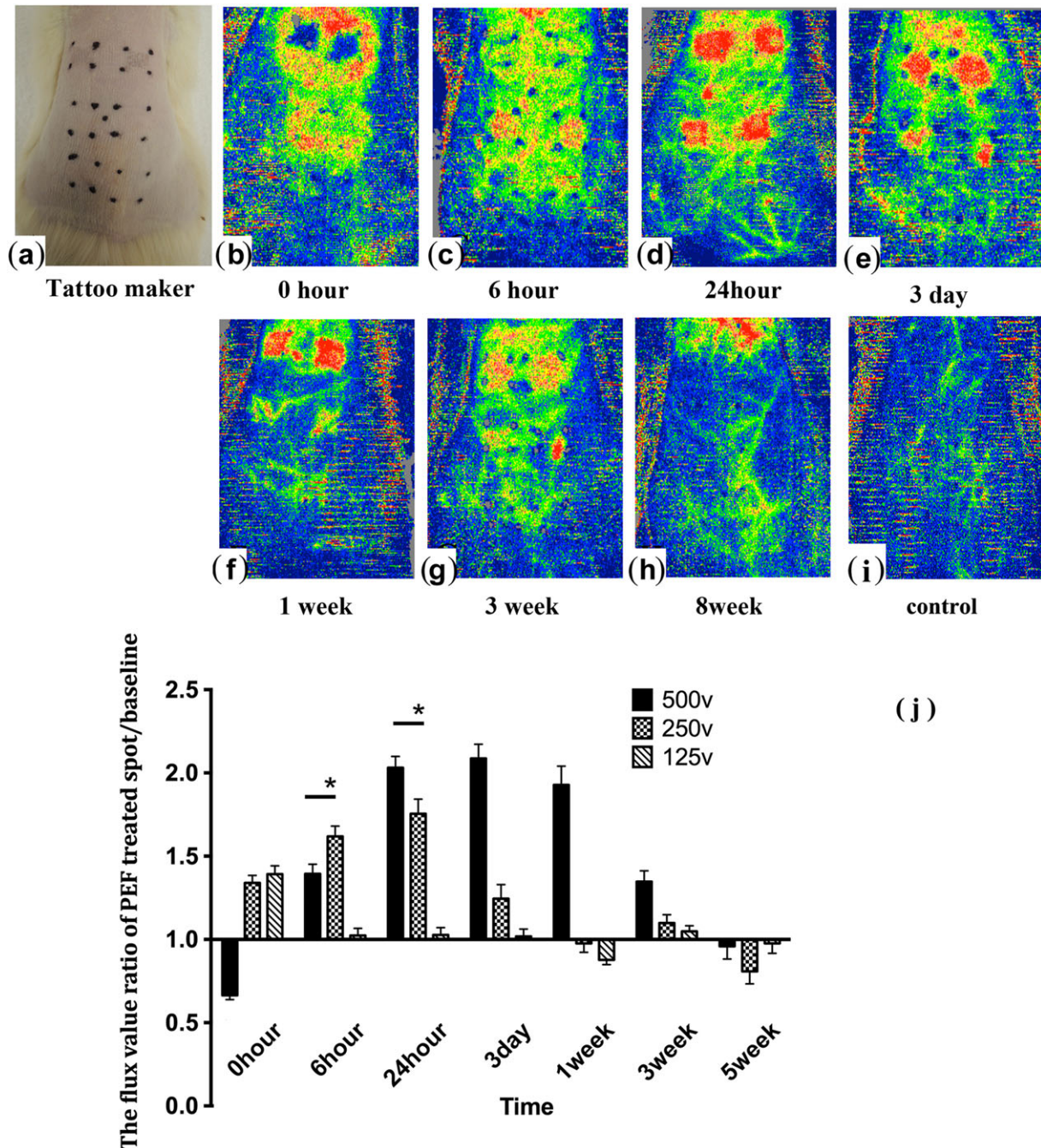


FIGURE 2 Laser Doppler scanning showed increased flow after partial irreversible electroporation (pIRE) treatment. (a) Six designated areas were treated with pIRE using contact electrodes with a surface area of 1 cm^2 . (b–i) A laser Doppler imager (Moor Instruments, Wilmington, DE) was used to assess blood flow. (j) Application of 500-V pulses eliminated the microcirculation in the treated area; however, 6 hr after pIRE administration, the blood flow increased significantly. This increased flow lasted 3 weeks after pIRE application. The application of pIRE at 250 and 125 V did not eliminate the microcirculation in the treated area but directly promoted blood flow. The increased flow lasted a shorter time than in the 500-V group. * p value < 0.05 [Colour figure can be viewed at wileyonlinelibrary.com]

3 | RESULTS

3.1 | Blood flow increase after pIRE administration

The application of 200 pulses of 500 V for $70 \mu\text{s}$ at 3 Hz eliminated the microcirculation at the treated area, but 6 hr after electric field administration, the detected flow increased by $39 \pm 6\%$ compared with the baseline levels (Figure 2). This increased flow in the pIRE-treated area reached a maximal level of $109 \pm 9\%$ 3 days after pIRE

administration. The flow was still $35 \pm 6\%$ higher in the treated area 3 weeks after pIRE application. The application of pIREs at 250 V did not eliminate the microcirculation in the treated area, as was the case for pIREs at 500 V. The detected flow increased $34 \pm 4\%$ compared with the baseline levels after the delivery. This increased flow in the pIRE-treated area reached a maximal level of $75 \pm 9\%$ 24 hr after pIRE administration. The flow reduced to baseline levels 1 week after treatment. Similar to the 250-V pIREs, the 125-V pIREs did not eliminate the microcirculation in the treated area. However, the flow

in the 125-V pIRE-treated area decreased to baseline levels 6 hr after treatment.

3.2 | Rat skin epidermis proliferation after pIRE administration

To get more details on the observed keratinocyte proliferation, we studied the expression levels of Ki-67, which regulate the proliferation and differentiation of mature keratinocyte (Endl & Gerdes, 2000). Ki-67 positively stained keratinocyte nuclei clearly differed from the negative, mitotically inactive blue-stained nuclei. The proliferation marker Ki-67 was found at a frequency of $28.37 \pm 2.48\%$, $28.74 \pm 2.57\%$, and $23.37 \pm 1.37\%$ for the keratinocytes in the 500-, 250-, and 125-V pIRE-treated areas, respectively, 1 day after pIRE administration,

whereas the frequency was $4.5 \pm 0.56\%$ for the untreated keratinocytes (Figure 3). The frequency of Ki-67 positively stained keratinocytes was still higher 3 weeks after pIRE administration in the 500-V pIRE-treated area, and the 250- and 125-V pIRE-treated areas still had a higher Ki-67 positively stained keratinocyte frequency 5 weeks after pIRE administration. The Ki-67 expression in the epidermis returned to basal levels 8 weeks after pIRE application (Figures S1 and S2).

Compared with the thickness in the control group, the thickness of the rat skin epidermis increased significantly in all sets 1 day after pIRE administration ($46.17 \pm 2.71 \mu\text{m}$ in the 500-V pIRE-treated skin, $44.56 \pm 2.16 \mu\text{m}$ in the 250-V pIRE-treated skin, and $36.42 \pm 2.40 \mu\text{m}$ in the 125-V pIRE-treated skin vs. $17.59 \pm 1.99 \mu\text{m}$ in the untreated skin; Figure 4). The epidermal thickening coincided with an increased number of epidermal cell layers and a more compact stratum corneum. Additionally, the rat skin of the 500-V pIRE-treated group exhibited

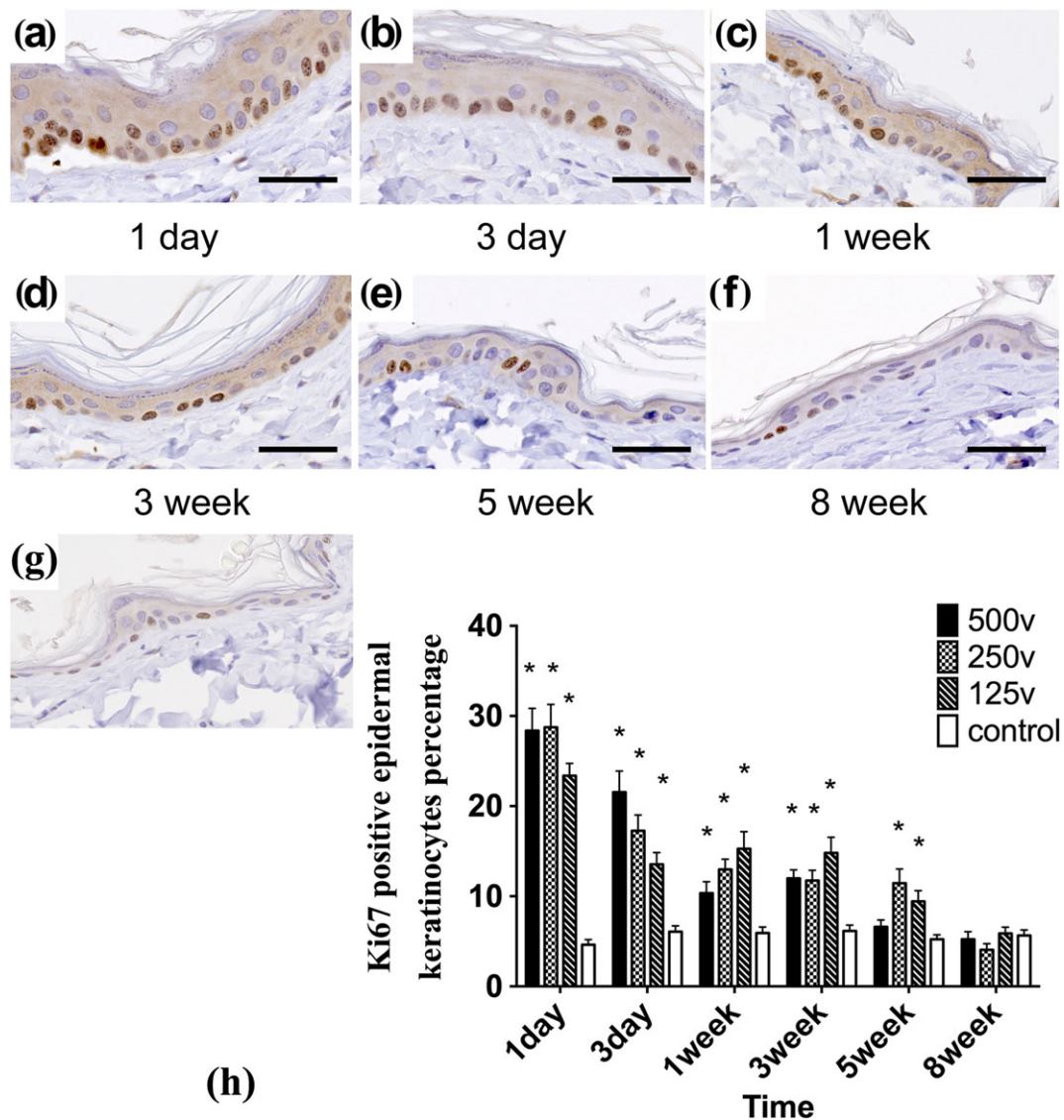


FIGURE 3 Impact of partial irreversible electroporation (pIRE) on Ki-67 expression levels in the epidermal keratinocytes. Images show the immunohistochemical staining of Ki-67 at various time points up to 2 months after the administration of 500-V pulsed electric fields (a-g). The plot shows that a higher frequency was present 3 weeks after pIRE administration in the 500-V pIRE-treated area, and the 250- and 125-V pIRE-treated areas still had a higher frequency of Ki-67-positive keratinocytes 5 weeks after pIRE administration. The Ki-67 expression in the epidermis returned to basal levels 8 weeks after pIRE application (h). The scale bar is 100 μm [Colour figure can be viewed at wileyonlinelibrary.com]

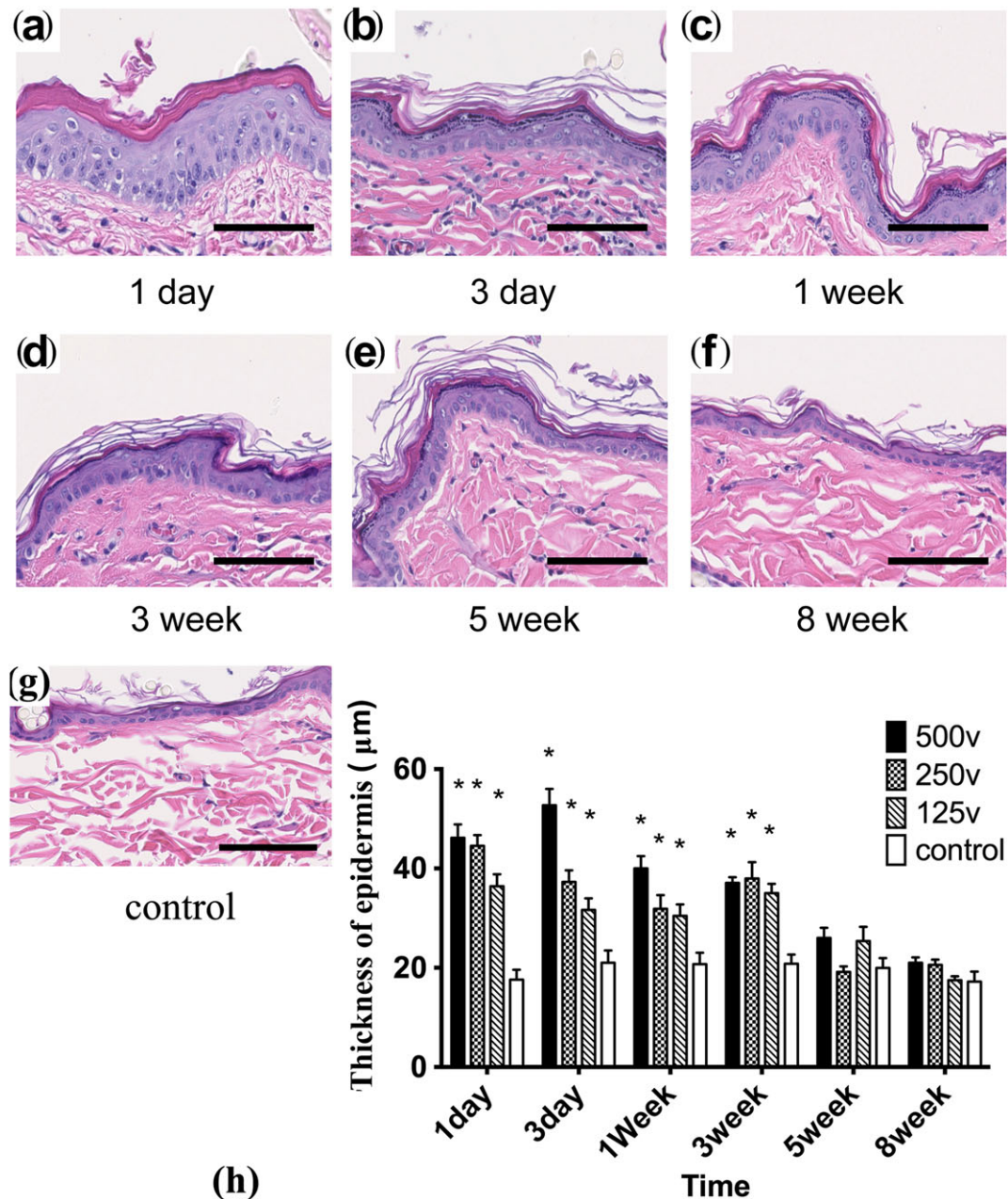


FIGURE 4 Dynamics of epidermal thickening and return to baseline levels. Images show haematoxylin and eosin staining of the 500-V pulsed electric field-treated epidermis (a–g). The plots show the average thickness of the epidermis and stratum corneum (h). The scale bar is 100 µm. **p* value < 0.05 compared with the control [Colour figure can be viewed at wileyonlinelibrary.com]

the highest increase. Three weeks after pIRE administration, the stratum corneum was normal, and the number of cell layers in the epidermis was reduced, although the epidermis was still thicker in the pIRE-treated areas of all sets than in the untreated skin (37.09 ± 1.14 µm in the 500-V pIRE-treated skin, 37.96 ± 3.30 µm in the 250-V pIRE-treated skin, and 35.04 ± 1.85 µm in the 125-V pIRE-treated skin vs. 20.81 ± 1.83 µm in the untreated skin). There were no differences among the three groups. Eight weeks after pIRE administration, the epidermis returned to their baseline thicknesses, similar to the untreated skin (21.02 ± 1.06 µm in the 500-V pIRE-treated skin, 20.58 ± 1.05 µm in the 250-V pIRE-treated skin, and 17.49 ± 0.79 µm in the 125-V pIRE-treated skin vs. 17.22 ± 2.01 µm in the untreated skin; Figures S3 and S4).

3.3 | Impact of pIREs on the dermal ECM

The total collagen protein levels in the 500- and 250-V pIRE-treated skin increased and were higher than those in the control group 3 days (35.28 ± 2.07 , 34.60 ± 1.41 , and 25.12 ± 1.23 µg/mg for 500-V, 250-V, and control groups, respectively) and 1 week (37.05 ± 2.24 , 38.36 ± 1.41 , and 26.57 ± 1.31 µg/mg for 500-V, 250-V, and control groups, respectively) after pIRE administration (Figure 5a). Both the 500- and 125-V pIRE-treated skin had higher total collagen protein levels than that in the control group (34.28 ± 1.14 , 34.28 ± 1.14 , and 26.13 ± 1.24 µg/mg for 500-V, 125-V, and control groups, respectively) 3 weeks after pIRE administration, whereas the 250-V pIRE group had a higher total collagen protein level even 5 weeks

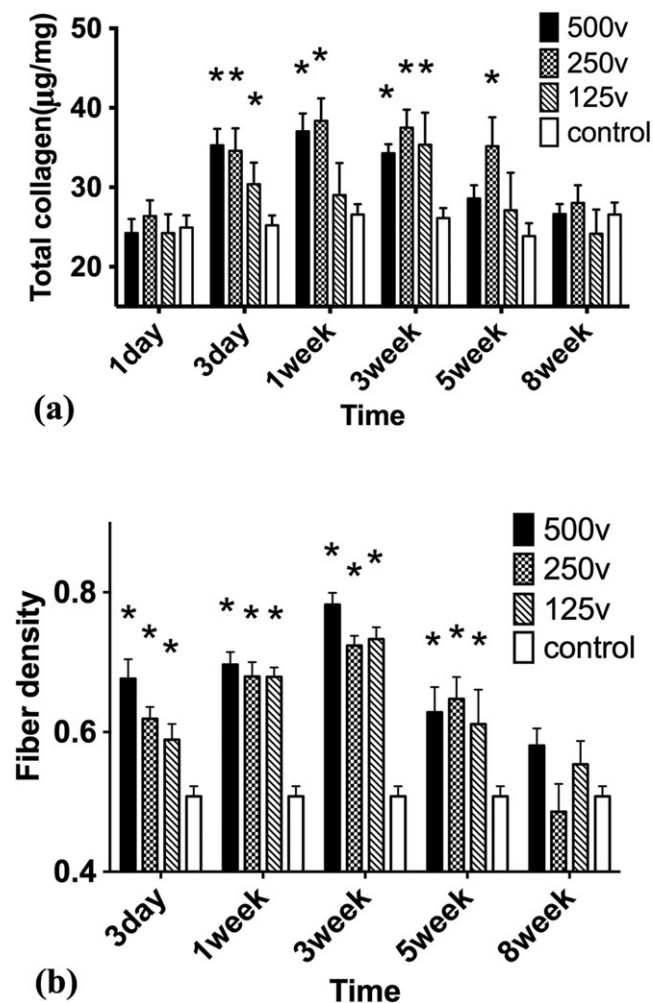


FIGURE 5 Impact of pulsed electric fields on dermal collagenesis and fibre density. (a) The total collagen protein levels in the pulsed electric field (PEF)-treated skin increased and were higher than those in the control group after PEF administration. (b) Quantitative analyses of the fibre density in the PEF-treated areas, which was significantly elevated. **p* value < 0.05 compared with the control

(35.17 ± 1.83 and 23.86 ± 1.62 µg/mg for 250-V and control groups, respectively) after pIRE administration. The total collagen protein levels in all sets decreased to baseline levels 8 weeks after treatment (26.63 ± 1.27, 28.03 ± 1.11, 24.16 ± 1.52, and 26.57 ± 1.51 µg/mg for 500-V, 250-V, 125-V, and control groups, respectively).

Using a previously developed image-processing algorithm, we quantified the fibre density and orientation in the histological sections (Quinn et al., 2014). An increase in the fibre density in the area of the 500- and 250-V pIRE-treated skin was clearly observed 3 days after the pIRE administration, and this increased fibre density in the pIRE-treated area in all sets reached a maximal increase 3 weeks after pIRE administration (0.687 ± 0.028 in the 500-V pIRE-treated skin, 0.619 ± 0.017 in the 250-V pIRE-treated skin, and 0.589 ± 0.022 in the 125-V pIRE-treated skin; Figure 5b). The collagen density then decreased after week 3. Two months after pIRE administration, the fibre density was not significantly different from that of the control tissue (0.580 ± 0.024 in the 500-V pIRE-treated skin, 0.486 ± 0.040 in the 250-V pIRE-treated skin, 0.554 ± 0.033 in the 125-V pIRE-

treated skin, and 0.508 ± 0.014 in the control group). Moreover, the fibre directional variance was not significantly different from that of the untreated skin with the exception of 3 weeks after pIRE administration, when the fibre directional variance in the 500- and 125-V pIRE-treated skin was lower than that in the control (Table S1, Figures S5–S7). These findings indicate that the pIRE process did not lead to the increased fibre alignment that is indicative of scar formation.

4 | DISCUSSION

Although the skin is incredibly durable and has an enormous regenerative capacity, eventually, skin cannot escape aging. Aged skin results in atrophy of skin components. However, the predominant feature of the aged dermis is the reduction and fragmentation of the extracellular collagen matrix; additionally, the turnover rate of the keratinocytes in the epidermis decreases considerably (Fisher et al., 2002).

Various techniques have been developed to achieve skin rejuvenation. Typically, resurfacing achieves the outcome of rejuvenation by destroying the epidermis and superficial papillary dermis of the skin. The subsequent establishment of newly formed collagen and a tightened skin appearance follows this removal. However, there is a wide range of significant side effects (Avram et al., 2009; Cox & Adigun, n.d.). The most frequent and concerning complications are scarring and dyspigmentation. Scarring often occurs because of the excessive thermal damage caused by the overlap of treatment areas.

More recently, we introduced a non-invasive, nonthermal technique to rejuvenate skin with pIRE (Golberg, Khan, et al., 2015). We tested pIRE in a young rat model, and the results showed that pIRE provides a promising low-cost, complication-free, and easy-to-adapt procedure, resulting in the induction of prominent proliferation of the epidermis, formation of microvasculature, secretion of new collagen, and increased metabolic activity. However, many more recent studies have investigated age-related alterations in the proliferative aspects of regeneration, including keratinocyte proliferation, ECM synthesis, and angiogenesis (de Melo Rambo et al., 2014; Reed et al., n.d.). Because aged humans are the main group who would like to receive cosmetic procedures to slow regeneration, we evaluated the effect of pIRE in skin rejuvenation with an aged animal model.

In this study, we evaluated the effect of pIRE in skin rejuvenation using an experimental model of aged rats. One of the intriguing results of this work is the difference in increasing thickness of epidermis timing between aged, measured here, and young rats, reported by us in Golberg, Khan, et al. (2015). In aged rats, we observed a prominent epidermal growth with a significant increase in the epidermal thickness after 1 day of the treatment. However, in the previous work (Golberg, Khan, et al., 2015), in younger rats, the treatment with 500 V resulted in focal necrosis followed by hyperkeratosis after 3 days. The differences in the timing of hyperkeratosis could be explained by the differences in the actual electric field applied to each cell. Although the same voltage was applied through the same electrodes at same gaps in the two studies, the electric properties of aged and young skin are different, as was shown in Peyman, Rezazadeh, and Gabriel (2001). These electric properties changes, which can be

attributed to water content (Peyman et al., 2001) and structural changes (Farage, Miller, Elsner, & Maibach, 2007), affect the distribution of the electric fields inside the skin, and, therefore, could change the local electric field strength to which specific cells are exposed to (Aström, Lemaire, & Wardell, 2012; Corovic et al., 2013; Golberg, Bruinsma, Uygun, & Yarmush, 2015). Exposure of cells to the different local electric field could lead to different responses (Golberg, Bei, Sheridan, & Yarmush, 2013).

The results of the proliferation marker Ki-67 showed that keratinocytes actively proliferated after pIRE was administered. The proliferating keratinocytes may be divided into two groups: "stem cells" with their highly proliferative potential and a subpopulation of uninjured keratinocytes. Future studies should provide more information on the levels and roles of each of subgroups in skin rejuvenation. pIRE induced re-epithelialization in aged rats without impairing the mechanical properties of the skin, stratum corneum, or ECM. Additionally, the thickness of the epidermis temporarily increased after pIRE administration and then returned to baseline 5 weeks after the treatment.

Skin aging is often associated with poor blood supply (Farage, Miller, & Maibach, 2010; Ryan, 2004; Tsuchida, 1993). We showed that pIRE treatment promoted blood flow in the aged rat skin. However, the applied voltage had different impacts on the blood flow change. According to our results, the application of 500-V pulses eliminated the microcirculation in the treated area; however, 6 hr after pIRE administration, the blood flow increased significantly, and this increased flow lasted 3 weeks after pIRE application. Perhaps the increased interstitial pressure and decreased intravascular pressure due to irreversible damage to vessels mediated the vasoconstriction phenomena (Mandel et al., 2013; Palanker, Vankov, Freyvert, & Huie, 2008). Our previous study showed that proangiogenesis factors, such as vascular endothelial growth factor, interleukin 10, and epidermal growth factor, were elevated, indicating that angiogenesis was induced at the pIRE-treated site (Golberg, Khan, et al., 2015). In addition, we showed the increased levels of nestin, angiogenesis marker, in the papillary dermal microvasculature, detected from 1 day to 3 weeks after PEF treatment (Golberg, Khan, et al., 2015). The application of pIREs at 250 and 125 V did not eliminate the microcirculation in the treated area but directly promoted blood flow. The increased flow lasted a shorter time than in the 500-V group. An explanation for the insignificant vasoconstriction phenomena in the 250- and 125-V groups may be that the low applied voltage cannot irreversibly damage vessels.

The creation of new, fine collagen may be the most important hallmark of skin rejuvenation. In our study, we did find significant evidence of the impact of pIRE on dermal ECM. Both the collagen protein and fibre density in the aged skin increased after pIRE administration. Moreover, on the basis of the image-processing algorithm, we found that the orientation of collagen fibres in the histological sections did not change, indicating a lack of scar formation in the treated area.

In the study, we tested three different PEF voltages; although the 500-V pIREs could promote the highest and most enduring blood flow, the different voltages did not have substantially different effects on re-epithelialization and collagenesis. Although the mechanisms of skin rejuvenation after the application of pIREs are complex and involve multiple pathways, no evidence showed that a higher voltage resulted in a better rejuvenation effect.

This study does have limitations. Although commonly used as a model for skin rejuvenation, rat skin is different from human skin. The effect of pIREs on human skin rejuvenation should be studied in clinical trials. Skin rejuvenation after pIRE administration is a multifactorial process. Therefore, further research is needed to elucidate the underlying molecular mechanism of various cell subpopulations responses to high-voltage PEFs. Furthermore, detailed electro-mechanical simulations of skin at various age and physiological conditions are needed to get a better understanding of local electric field distribution, which is critical to understand cell response.

In conclusion, we demonstrate that this novel non-invasive approach effectively achieves keratinocyte proliferation, ECM synthesis, and angiogenesis in an aged rat model. We show that age plays an important role in skin response to external PEFs.

ACKNOWLEDGEMENTS

We acknowledge the Shriners Grant 85120-BOS and the United States-Israel Binational Science Foundation (BSF) for supporting this study. We thank the Dana-Farber/Harvard Cancer Center in Boston, MA, for the use of the Rodent Histopathology Core, which provided histological services for this project. The Dana-Farber/Harvard Cancer Center is supported in part by the NCI Cancer Center Support Grant NIH 5 P30 CA06516. X. L. acknowledges support from the National Natural Science Foundation of China (No. 81402574).

AUTHORS CONTRIBUTIONS

X.L. did the experiments, analysed the data, and drafted the manuscript. N.S. did the experiments and analysed the data. M.W. analysed the data and edited the manuscript. H.A. did the histological part the study. J.D.J. and K.P.Q. did the quantitative analysis of histology. W. G.A. conceived the study and reviewed the manuscript. A.G. conceived the study, developed the EP protocols, analysed the data, and drafted the manuscripts. M.L.Y. conceived the study and reviewed the data and the manuscript.

CONFLICTS OF INTEREST

The authors have declared that there is no conflict of interest.

ORCID

Alexander Golberg  <http://orcid.org/0000-0001-8782-8879>

REFERENCES

- ASDS, (2016). ASDS survey: Nearly 10.6 million treatments performed in 2016. [accessed 30 June 2017]. <http://www.crossroadstoday.com/story/35550117/asds-survey-nearly-105-million-treatments-performed-in-2016>
- Aström, M., Lemaire, J. J., & Wardell, K. (2012). Influence of heterogeneous and anisotropic tissue conductivity on electric field distribution in deep brain stimulation. *Medical and Biological Engineering and Computing*, 50(1), 23–32. <https://doi.org/10.1007/s11517-011-0842-z>
- Avram, M. M., Tope, W. D., Yu, T., Szachowicz, E., & Nelson, J. S. (2009). Hypertrophic scarring of the neck following ablative fractional carbon dioxide laser resurfacing. *Lasers in Surgery and Medicine*, 41, 185–188. <https://doi.org/10.1002/lsm.20755>
- Badin, A. Z. D., Casagrande, C., Roberts III, T., Saltz, R., Moraes, L. M., Santiago, M., & Chiaratti, M. G. (2001). Minimally invasive facial

- rejuvenation endolaser mid-face lift. *Aesthetic Plastic Surgery*, 25(6), 447–453. <https://doi.org/10.1007/s00266-001-0023-9>
- Bourguignon, G. J., Jy, W., & Bourguignon, L. Y. W. (1989). Electric stimulation of human fibroblasts causes an increase in Ca^{2+} influx and the exposure of additional insulin receptors. *Journal of Cellular Physiology*, 140(2), 379–385. <https://doi.org/10.1002/jcp.1041400224>
- Corovic, S., Lackovic, I., Sustaric, P., Sustar, T., Rodic, T., & Miklavcic, D. (2013). Modeling of electric field distribution in tissues during electroporation. *Biomedical Engineering Online*, 12(1), 16. <https://doi.org/10.1186/1475-925X-12-16>
- Cox, S. E., & Adigun, C. G. Complications of injectable fillers and neurotoxins. *Dermatologic Therapy*, 24(6), 524–536. Available at: <http://www.ncbi.nlm.nih.gov/pubmed/22515668> Accessed August 19, 2014. <https://doi.org/10.1111/j.1529-8019.2012.01455.x>
- Davalos, R. V., Mir, L. M., & Rubinsky, B. (2005). Tissue ablation with irreversible electroporation. *Annals of Biomedical Engineering*, 33(2), 223–231. <https://doi.org/10.1007/s10439-005-8981-8>
- de Melo Rambo, C. S., Silva, J. A. Jr, Serra, A. J., Ligeiro, A. P., Vieira, R. P., Albertini, R., ... de Tarso Camillo de Carvalho, P. (2014). Comparative analysis of low-level laser therapy (660 nm) on inflammatory biomarker expression during the skin wound-repair process in young and aged rats. *Lasers in Medical Science*, 29(5), 1723–1733. <https://doi.org/10.1007/s10103-014-1582-8>
- Endl, E., & Gerdes, J. (2000). The Ki-67 protein: Fascinating forms and an unknown function. *Experimental Cell Research*, 257(2), 231–237. <https://doi.org/10.1006/excr.2000.4888>
- Farage, M. A., Miller, K. W., Elsner, P., & Maibach, H. I. (2007). Structural characteristics of the aging skin: A review. *Cutaneous and Ocular Toxicology*, 26(4), 343–357. <https://doi.org/10.1080/15569520701622951>
- Farage, M.A., Miller, K.W. & Maibach, H.I., 2010. *Textbook of aging skin*, <https://doi.org/10.1007/978-3-540-89656-2>,
- Fernandes, J. R., Samayoa, J. C., Broelsch, G. F., McCormack, M. C., Nicholls, A. M., Randolph, M. A., ... Austen, W. G. Jr. (2013). Micro-mechanical fractional skin rejuvenation. *Plastic and Reconstructive Surgery*, 131, 216–223. Available at: <http://www.ncbi.nlm.nih.gov/pubmed/23357983>. <https://doi.org/10.1097/PRS.0b013e3182789afa>
- Fisher, G. J., Kang, S., Varani, J., Bata-Csorgo, Z., Wan, Y., Datta, S., & Voorhees, J. J. (2002). Mechanisms of photoaging and chronological skin aging. *Archives of Dermatology*, 138(11). <https://doi.org/10.1001/archderm.138.11.1462>
- Gibot, L., & Golberg, A. (2016). Electroporation in scars/wound healing and skin response. In *Handbook of electroporation* (pp. 1–18). Available at: https://doi.org/10.1007/978-3-319-26779-1_64-1 Accessed July 2, 2017. Cham: Springer international publishing.
- Golberg, A., Bei, M., Sheridan, R. L., & Yarmush, M. L. (2013). Regeneration and control of human fibroblast cell density by intermittently delivered pulsed electric fields. *Biotechnology and Bioengineering*, 110(6), 1759–1768. <https://doi.org/10.1002/bit.24831>
- Golberg, A., Broelsch, G. F., Bohr, S., Mihm, M. C., Austen, W. G., Albadawi, H., ... Yarmush, M. L. (2013). Non-thermal, pulsed electric field cell ablation: A novel tool for regenerative medicine and scarless skin regeneration. *Technology*, 1(1), 1–8. Available at: <http://www.pubmedcentral.nih.gov/articlerender.fcgi?artid=4078877&tool=pmcentrez&rendertype=abstract>. Accessed August 19, 2014
- Golberg, A., Bruinsma, B. G., Jaramillo, M., Yarmush, M. L., & Uygun, B. E. (2016). Rat liver regeneration following ablation with irreversible electroporation. *PeerJ*, 4, e1571. <https://doi.org/10.7717/peerj.1571>
- Golberg, A., Bruinsma, B. G., Uygun, B. E., & Yarmush, M. L. (2015). Tissue heterogeneity in structure and conductivity contribute to cell survival during irreversible electroporation ablation by “electric field sinks”. *Scientific Reports*, 5, 8485. Available at: <http://www.nature.com/srep/2015/150216/srep08485/full/srep08485.html>. Accessed August 3, 2015
- Golberg, A., Khan, S., Belov, V., Quinn, K. P., Albadawi, H., Felix Broelsch, G., ... Yarmush, M. L. (2015). Skin rejuvenation with non-invasive pulsed electric fields. *Scientific Reports*, 5, 10187. Available at: <http://www.nature.com/srep/2015/150512/srep10187/full/srep10187.html>. <https://doi.org/10.1038/srep10187> Accessed May 16, 2015
- Golberg, A., Villiger, M., Felix Broelsch, G., Quinn, K. P., Albadawi, H., Khan, S., ... Yarmush, M. L. (2017). Skin regeneration with all accessory organs following ablation with irreversible electroporation. *Journal of Tissue Engineering and Regenerative Medicine*, 12, 98–113. Available at: <https://doi.org/10.1002/term.2374>, Accessed June 30, 2017
- Golberg, A., Villiger, M., Khan, S., Quinn, K. P., Lo, W. C. Y., Bouma, B. E., ... Yarmush, M. L. (2016). Preventing scars after injury with partial irreversible electroporation. *The Journal of Investigative Dermatology*, 136(11), 2297–2304. <https://doi.org/10.1016/j.jid.2016.06.620>
- Hoening, J., & Hoening, D. (2013). Minimally invasive periorbital rejuvenation. *Facial Plastic Surgery*, 29(4), 295–309. <https://doi.org/10.1055/s-0033-1349363>
- Lee, H. J., Lee, E. G., Kang, S., Sung, J. H., Chung, H. M., & Kim, D. H. (2014). Efficacy of microneedling plus human stem cell conditioned medium for skin rejuvenation: A randomized, controlled, blinded split-face study. *Annals of Dermatology*, 26(5), 584–591. <https://doi.org/10.5021/ad.2014.26.5.584>
- Mandel, Y., Manivanh, R., Dalal, R., Huie, P., Wang, J., Brinton, M., & Palanker, D. (2013). Vasoconstriction by electrical stimulation: New approach to control of non-compressible hemorrhage. *Scientific Reports*, 3, 2111. Available at: <http://www.nature.com/srep/2013/130704/srep02111/full/srep02111.html>. Accessed January 24, 2015
- Mulholland, R. S. (2011). Radio frequency energy for non-invasive and minimally invasive skin tightening. *Clinics in Plastic Surgery*, 38(3), 437–448. <https://doi.org/10.1016/j.cps.2011.05.003>
- Nand, P., & Riyal, P. (2014). Skin ageing and its remedies: A review. *Hygeia*, 6(1), 1–5.
- Neumann, E., & Rosenheck, K. (1972). Permeability changes induced by electric impulses in vesicular membranes. *The Journal of Membrane Biology*, 10(3), 279–290. Available at: <http://www.ncbi.nlm.nih.gov/pubmed/4667921>. <https://doi.org/10.1007/BF01867861>
- Palanker, D., Vankov, A., Freyvert, Y., & Huie, P. (2008). Pulsed electrical stimulation for control of vasculature: Temporary vasoconstriction and permanent thrombosis. *Bioelectromagnetics*, 29(2), 100–107. Available at: <http://www.ncbi.nlm.nih.gov/pubmed/17918191>. Accessed January 24, 2015
- Park, M., Ahn, J., Choi, Y., Kim, M., & Lee, J. (2012). The safety and efficacy of a combined diode laser and bipolar radiofrequency compared with combined infrared light and bipolar radiofrequency for skin rejuvenation. *Indian Journal of Dermatology, Venereology and Leprology*, 78(2), 146. Available at: <http://www.ncbi.nlm.nih.gov/pubmed/22421644>. Accessed June 30, 2017
- Pavšelj, N., & Miklavčič, D. (2008). A numerical model of permeabilized skin with local transport regions. *IEEE Transactions on Biomedical Engineering*, 55, 1927–1930. <https://doi.org/10.1109/TBME.2008.919730>
- Peyman, A., Rezazadeh, A. A., & Gabriel, C. (2001). Changes in the dielectric properties of rat tissue as a function of age at microwave frequencies. *Physics in Medicine and Biology*, 46(6), 1617–1629. <https://doi.org/10.1088/0031-9155/46/6/303>
- Phillips, M., A., Narayan, R., Padath, T., Rubinsky, B. (2012). Irreversible electroporation on the small intestine. *British Journal of Cancer*, 106(3), 490–495. <https://doi.org/10.1038/bjc.2011.582>
- Quan, T., & Fisher, G. J. (2015). Role of age-associated alterations of the dermal extracellular matrix microenvironment in human skin aging: A mini-review. *Gerontology*, 61(5), 427–434. Available at: <http://www.ncbi.nlm.nih.gov/pubmed/25660807>. Accessed June 30, 2017
- Quinn, K. P., Golberg, A., Broelsch, G. F., Khan, S., Villiger, M., Bouma, B., ... Georgakoudi, I. (2014). An automated image processing method to quantify collagen fibre organization within cutaneous scar tissue. *Experimental Dermatology*, 24(1), 78–80. Available at: <http://www.ncbi.nlm.nih.gov/pubmed/25256009>. Accessed March 12, 2015
- Reed, M. J., Karres, N., Eyman, D., Vernon, R. B., & Edelberg, J. M. (n.d.). Age-related differences in repair of dermal wounds and myocardial infarcts attenuate during the later stages of healing. *In vivo* (Athens,

- Greece), 20(6B), pp.801–6. Available at: <http://www.ncbi.nlm.nih.gov/pubmed/17203771> [Accessed June 30, 2017].
- Rubinsky, B., Onik, G., & Mikus, P. (2007). Irreversible electroporation: a new ablation modality—Clinical implications. *Technology in Cancer Research & Treatment*, 6, 37–48. <https://doi.org/10.1177/153303460700600106>
- Ryan, T. (2004). The ageing of the blood supply and the lymphatic drainage of the skin. *Micron*, 35(3), 161–171. <https://doi.org/10.1016/j.micron.2003.11.010>
- Savoia, A., Landi, S., & Baldi, A. (2013). A new minimally invasive mesotherapy technique for facial rejuvenation. *Dermatology and Therapy*, 3(1), 83–93. <https://doi.org/10.1007/s13555-012-0018-2>
- Seo, K. Y., Kim, D. H., Lee, S. E., Yoon, M. S., & Lee, H. J. (2013). Skin rejuvenation by microneedle fractional radiofrequency and a human stem cell conditioned medium in Asian skin: A randomized controlled investigator blinded split-face study. *Journal of Cosmetic and Laser Therapy*, 15(1), 25–33. <https://doi.org/10.3109/14764172.2012.748201>
- Tsuchida, Y. (1993). The effect of aging and arteriosclerosis on human skin blood flow. *Journal of Dermatological Science*, 5(3), 175–181. [https://doi.org/10.1016/0923-1811\(93\)90764-G](https://doi.org/10.1016/0923-1811(93)90764-G)
- Yarmush, M. L., Golberg, A., Serša, G., Kotnik, T., & Miklavčič, D. (2014). Electroporation-based technologies for medicine: Principles, applications, and challenges. *Annual Review of Biomedical Engineering*, 16, 295–320. Available at: <https://doi.org/10.1146/annurev-bioeng-071813-104622?journalCode=bioeng>. Accessed July 12, 2014
- Table S1.** Quantitative analyses showed no significant difference in fiber alignment, indicating a lack of scar formation in PEF-treated areas.
- Figure S1.** Representative images of Ki63 stained epidermis (a-f) in 250 V group. The scale bar is 100 μm .
- Figure S2.** Representative images of Ki63 stained epidermis (a-f) in 125 V group. The scale bar is 100 μm
- Figure S3.** Representative images of H&E stained epidermis (a-f) in 250 V Group. The scale bar is 100 μm .
- Figure S4.** Representative images of H&E stained epidermis (a-f). The scale bar is 100 μm .
- Figure S5.** Representative images of Trichrome-stained skin sections in 500 V group. The scale bar is 100 μm .
- Figure S6.** Representative images of Trichrome-stained skin sections in 250 V group. The scale bar is 200 μm .
- Figure S7.** Representative images of Trichrome-stained skin sections in 125 V group. The scale bar is 200 μm .

SUPPORTING INFORMATION

Additional supporting information may be found online in the Supporting Information section at the end of the article.

How to cite this article: Li X, Saeidi N, Villiger M, et al. Rejuvenation of aged rat skin with pulsed electric fields. *J Tissue Eng Regen Med*. 2018;12:2309–2318. <https://doi.org/10.1002/term.2763>